

Electronic structure of amorphous Si-N compounds

M. M. Guraya, H. Ascolani, and G. Zampieri

Comisión Nacional de Energía Atómica, Centro Atómico Bariloche e Instituto Balseiro, 8400 Bariloche, Argentina

J. H. Dias da Silva,* M. P. Cantão, and J. I. Cisneros

*Instituto de Física "Gleb Wataghin," Universidade Estadual de Campinas, Unicamp
13083-970 Campinas, São Paulo, Brazil*

(Received 14 October 1993)

We have measured valence-band photoemission spectra and dark conductivity of a -SiN $_x$:H compounds for compositions between $x = 0$ and $x = 1.35$. The photoemission spectra have been measured with Zr $M\zeta$ and Al $K\alpha$ radiation of 151.4 and 1486.6 eV, respectively. At $h\nu = 151.4$ eV the spectra resemble directly the total density-of-states (DOS) of the system; the most important change with x is the shift of spectral weight from near the valence-band maximum (VBM) toward the center of the band, indicating the change from a band of Si-Si bonding states to a band of Si-N bonding states. At $h\nu = 1486.6$ eV the spectra are dominated by the contribution of the Si-3s partial DOS; this contribution is located at the bottom of the band and shifts toward higher binding energies with increasing x . We compare our results at $x = 0.36$ and $x = 1.35$ with those of two recent calculations. Combining results of the dark-conductivity measurements and the photoemission spectra with a previous determination of the optical gaps we make a plot of the VBM, Fermi-level position, and conduction-band minimum (CBM) versus x . It is shown that the sudden opening of the gap at $x \sim 1$ is due mainly to the recession of the CBM.

I. INTRODUCTION

The amorphous system a -SiN $_x$ is attracting a great deal of attention because of its applications in the electronics industry and because it can be prepared in a wide range of concentrations x , allowing the study of the properties as they evolve from semiconducting amorphous silicon ($x = 0$) to insulating amorphous silicon nitride ($x = 4/3$).

The preparation methods include chemical-vapor deposition (CVD) of NH $_3$ -SiH $_4$ or NH $_3$ -SiCl $_4$ gas mixtures at high temperatures (~ 1000 °C),¹⁻³ glow discharge or plasma-enhanced CVD of NH $_3$ -SiH $_4$ or N $_2$ -SiH $_4$ gas mixtures at lower temperatures (~ 300 °C),⁴⁻⁹ and dc or RF sputtering of Si in a N $_2$ -containing atmosphere.¹⁰⁻¹² Atomic H is generally present in the films in concentrations between 5 and 40 at. %, although films without H have also been prepared by sputtering of Si in a hydrogen-free atmosphere.¹⁰

Several experimental and theoretical studies of the bonding and electronic structure of this system have been reported in the past years. The experimental studies of the bonding structure have included x-ray diffraction,¹ neutron diffraction,² IR absorption,^{5,11-13} Auger electron spectroscopy,^{6,8} and core-level photoemission spectroscopy.^{3,6,8-11,13,14} All these experiments support a random bonding model in which the Si atoms occupy tetrahedral sites with Si, N, or H atoms as first neighbors, while N atoms are in a threefold planar configuration bound to three Si atoms at low x and to Si, H, or N atoms at high x .

The electronic structure of these alloys is mainly covalent with the valence band (VB) being formed by Si-

Si bonding states derived from the interaction of sp^3 hybrids on Si atoms, Si-N bonding states derived from the interaction of sp^3 and sp^2 hybrids on adjacent Si and N atoms, and N $2p_z$ nonbonding states. The experimental studies have included optical absorption in the visible and ultraviolet regions,^{4,5,7,12} VB photoemission spectroscopy,^{3,8-10,13} and inverse photoemission spectroscopy.⁸ On the theoretical side, the first calculations of the VB were made for the α and β phases of crystalline silicon nitride^{15,16} and for amorphous Si $_3$ N $_4$.¹⁷ Only recently have there appeared studies of the electronic structure at nonstoichiometric compositions.¹⁸⁻²¹

In the present paper we report results of dark-conductivity measurements and of VB photoemission spectroscopy of a -SiN $_x$:H films with x between 0 and 1.35. This work completes our previous study of the bonding structure of these films.¹³ By combining results of different techniques we make a plot of the band edges and the Fermi level position in the pseudogap as a function of the N content x . We also present a comparison of our VB photoemission spectra at $x = 0.36$ and $x = 1.35$ with spectra made out of the calculations of Robertson,²⁰ and of Ordejón and Ynduráin.²¹

II. EXPERIMENT

The samples were prepared by RF sputtering of Si in an atmosphere of N $_2$, H $_2$, and Ar. The total pressure of the gas mixture was fixed at 1.5 Pa, the hydrogen flux was kept constant at 11 sccm (cubic centimeter per minute at STP), and the N $_2$ partial pressure was varied between 0 and 0.1 Pa. The substrate temperature was 180 °C

and the RF power was 200 W. The optical gap was determined from transmission in the absorption edge and nearby regions using a DMR-21 Zeiss spectrophotometer. More details about the preparation method and the determination of the optical gap can be found in Dias da Silva *et al.*¹²

The curves of dark conductivity versus temperature were measured in vacuum at a pressure of 10^{-4} Torr. A microcomputer with AD/DA interfaces was used for the data acquisition and to control the applied voltage and the rate of heating ($1^\circ\text{C}/\text{min}$).

The photoemission experiments were performed in an UHV chamber (base pressure of 10^{-10} Torr) equipped with an hemispherical electrostatic energy analyzer and a standard twin-anode x-ray gun. We used two x-ray lines: Zr $M\zeta$ and Al $K\alpha$ of $h\nu=151.4$ and 1486.6 eV, respectively. The full width at half maximum (FWHM) of the Si $2p$ peak measured in *c* Si was 1.65 eV with both x-ray lines; allowing for the 0.6 eV energy separation between the $2p_{3/2}$ and $2p_{1/2}$ components and the 0.21 eV broadening due to the core-hole lifetimes²² we derive an instrumental broadening of 1.4 eV. Prior to the measurements the samples were cleaned by mild Ar sputtering to remove O and C contaminants present on the surface; preferential sputtering of N was not observed in agreement with our previous study.¹³ As the samples showed signs of charging, we adopted the procedure of referencing all the energies to that of photoelectrons emitted from the Ar $2p_{3/2}$ level,²³ to which we assigned a constant binding energy of 243 eV. Note that with this procedure we avoid the charging effects but at the cost of losing the information on the position of the Fermi level within the band gap.

III. RESULTS AND DISCUSSION

Figure 1 shows the results of the dark-conductivity measurements for all the samples with $x < 1$. It is seen that the conductivity decreases strongly with the incor-

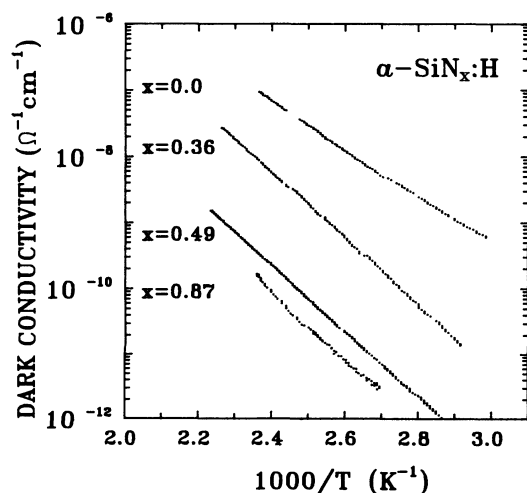


FIG. 1. Temperature dependence of the dark conductivity for the samples with $x < 1$.

poration of N. The results corresponding to the samples with $x > 1$ are not included because the conductivities were below the detectability limit of the apparatus over most of the temperature range. All the curves in Fig. 1 fall linearly over at least two orders of magnitude indicating well defined activation energies. Following previous studies^{7,24} we assume that the majority carriers are electrons, and therefore that the activation energies correspond to the energy separation between the conduction-band minimum (CBM) and the Fermi level. These activation energies will be used below to locate the Fermi levels in the band gaps.

The Si $2p$ spectra excited with $h\nu = 151.4$ or 1486.6 eV showed chemical shifts and asymmetric line shapes as reported earlier.¹³ The N $1s$ spectra (accessible with $h\nu = 1486.6$ eV only) were also measured to verify the compositions, which agreed within 20% with the compositions published in our previous work.

The compositions, optical gaps, and activation energies are listed in Table I.

The VB photoemission spectra are shown in Figs. 2 and 3. The energy zeros were determined by assigning a binding energy of 243 eV to the Ar $2p_{3/2}$ peaks measured in each sample. In the spectra of Fig. 2, taken at $h\nu = 1486.6$ eV, two characteristic structures separated by a gap of ~ 4.5 eV are observed. The peak at ~ 20 eV, which grows in intensity with the N content, has almost exclusively N $2s$ character. The other structure, between 0 and 15 eV, comprises the Si $3s$, Si $3p$, and N $2p$ contributions; it is seen that the spectra have maximum intensity at the bottom of this upper VB, and that this maximum shifts toward higher binding energies when x increases, closing the gap between the two structures. It will be shown below that the maximum in the upper VB corresponds to the Si $3s$ partial density of states (DOS), which is enhanced at this high photon energy.

Figure 3 shows the spectra taken at $h\nu = 151.4$ eV. Only the upper VB is shown because a spurious line of the Zr anode (C $K\alpha$, $h\nu = 278$ eV) produced a broad peak of Si $2s$ photoelectrons right at the energies where the N $2s$ structure should appear. The most important change seen in the spectra when x increases is the shift of spectral weight from near the valence-band maximum (VBM) towards the center of the band. As these photoemission spectra should resemble directly the total DOS's (see below), we assign the prominent feature near the VBM at $x = 0$ to the band of Si-Si bonding states, and the main feature at the center of the VB at $x = 1.35$ to the band of Si-N bonding states. The maximum of the

TABLE I. Compositions, optical gaps, and activation energies.

x	E_g (eV)	E_a (eV)
0.	1.89	0.72
0.36	2.03	0.91
0.49	2.11	0.99
0.87	2.56	1.0
1.11	4.21	
1.35	5.16	

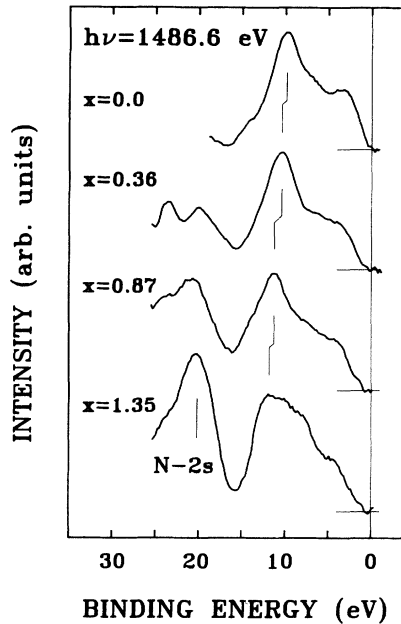


FIG. 2. Valence-band photoemission spectra of $a\text{-SiN}_x\text{:H}$ taken at $h\nu = 1486.6$ eV.

band corresponding to the heteropolar Si-N bonds lies at 5.7 eV higher binding energy than the maximum of the band corresponding to the homopolar Si-Si bonds. The peak near the VBM at $x = 0.87$ is thought to have contributions from Si-Si bonding states and from N $2p_z$ nonbonding states; at higher N contents the band of Si-Si bonding states disappears and the band of N $2p_z$ nonbonding states increases giving rise to the shoulder at 5.3 eV in the spectra at $x = 1.35$.

Combining the VBM's determined from the photoe-

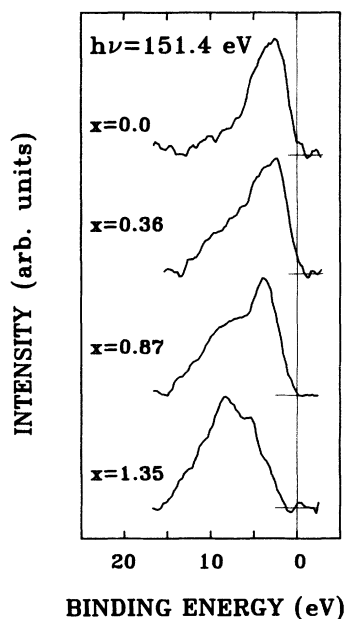


FIG. 3. Valence-band photoemission spectra of $a\text{-SiN}_x\text{:H}$ taken at $h\nu = 151.4$ eV.

mission experiments with the optical gaps and activation energies of Table I we have built the plot of the band edges and the Fermi-level position shown in Fig. 4. Starting with the positions of the VBM's (relative to the Ar $2p_{3/2}$ level) we have added the optical gaps to obtain the CBM's, and from these we have subtracted the activation energies to obtain the Fermi-level positions. The full line corresponding to the VBM is a quadratic fit to the VBM's at $x = 0, 0.36, 0.87,$ and 1.35 ; we have used this curve to locate the VBM's of the samples with $x = 0.49$ and 1.11 (not measured). The full lines corresponding to the Fermi level and CBM have been drawn to guide the eye and have no other meaning. It is seen that the sudden opening of the gap at $x \sim 1$ is due mainly to the sudden recession of the CBM, the change of the VBM being comparatively smoother. The inset shows that the sudden change of the CBM can be correlated with the falling below one of the mean number of Si neighbors of a Si atom. This observation confirms the interpretation of the opening of the gap in terms of a percolation transition: as long as Si-Si extended paths exist in the alloys the band edges are determined by Si-Si bonding and antibonding states separated by ~ 2 eV; when the incorporation of N prevents the formation of these extended Si-Si paths, the CBM becomes determined by Si-N antibonding states, which lie ~ 2 eV higher in energy, and the VBM becomes determined by the N $2p_z$ nonbonding states, which lie slightly below the band of Si-Si bonding states and above the band of Si-N bonding states.

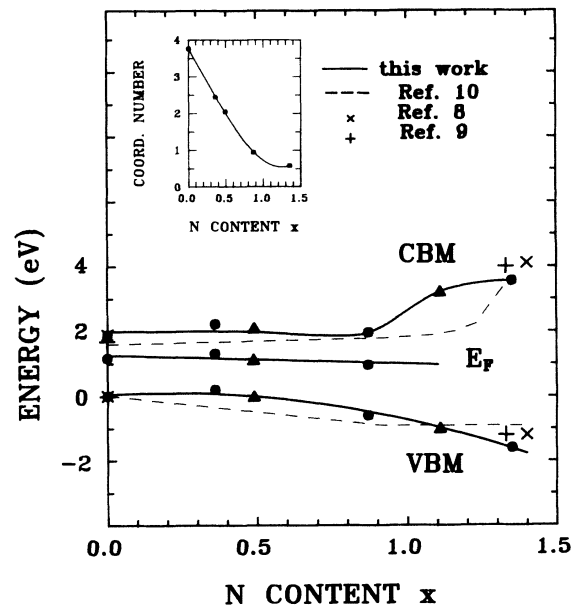


FIG. 4. Plot of the valence-band edges and the Fermi-level position as a function of the N content x . The circles correspond to those samples for which VB photoemission, optical gap, and activation energy have been measured. The triangles correspond to those samples for which only optical gap and activation energy have been determined. The inset shows the mean number of Si neighbors of a Si atom as a function of the N content, determined for this same set of samples in a previous work (Ref. 13).

Also shown in Fig. 4 are results reported by other authors. Our locations of the band edges at $x = 0$ and $x \approx 1.33$ are totally consistent with those found by Iqbal *et al.*⁸ and by Yang *et al.*⁹ in their studies of a -Si:H/ a -SiN_{*x*}:H heterojunctions. The small discrepancies, which are within the experimental error, can also be attributed to differences in the films due to the different preparation methods. Regarding the comparison with the results of Kärcher, Ley, and Johnson¹⁰ we find that the main differences are in the behavior of the CBM: the sudden change of the CBM occurs before in our curve and is less dramatic than in the curve of Kärcher, Ley, and Johnson. Since the films were prepared by the sputtering method in both cases, the origin of the discrepancy is likely to be due to the choice of different reference levels (N 1s and Ar 2p_{3/2}) and/or the use in Ref. 10 of optical gaps reported by Kurata, Hirose, and Osaka⁴ for glow-discharge a -SiN_{*x*}:H. It has been shown recently that the N 1s level undergoes a chemical shift towards higher binding energies when x increases,^{3,6,13} and therefore it cannot be taken as a constant level. When we refer our data to the N 1s level instead of the Ar 2p_{3/2} level both the VBM and the CBM shift upwards in energy and the opening of the gap results more asymmetric as in the work of Kärcher, Ley, and Johnson.

In Figs. 5 and 6 we compare our VB photoemission spectra with spectra made out of the calculations of Robertson²⁰ and of Ordejón and Ynduráin.²¹ Robertson (R) calculated the electronic structure of β -Si₃N₄ and of a series of crystalline models of SiN_{*x*} using a tight-binding method with parameters optimized to fit the optical gap and the VB photoemission spectra of Kärcher, Ley, and Johnson.¹⁰ Ordejón and Ynduráin (OY) calculated the electronic structure of Bethe lattices of Si and N atoms by the average Green's function method with parameters

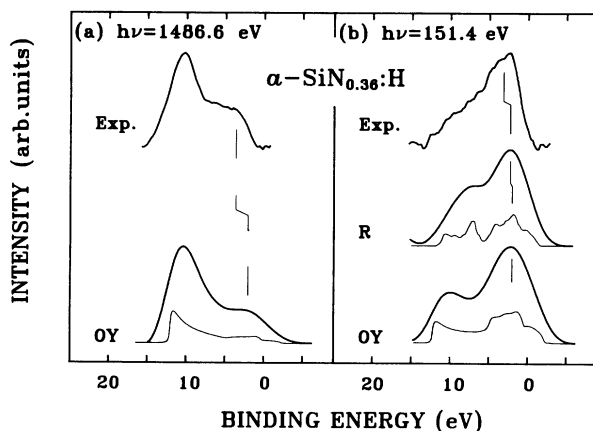


FIG. 5. (a) Comparison of experimental (Exp.) and calculated (OY) photoemission spectra at $h\nu = 1486.6$ eV. (b) Comparison of the experimental photoemission spectrum taken at $h\nu = 151.4$ eV (Exp.) with the total DOS's calculated by Robertson (R) (Ref. 20) and by Ordejón and Ynduráin (OY) (Ref. 21). The experimental spectra correspond to $x = 0.36$ and the calculations to $x = 0.4$ (R) and $x = 0.33$ (OY). The unbrodened theoretical curves are also shown in a smaller ordinate scale.

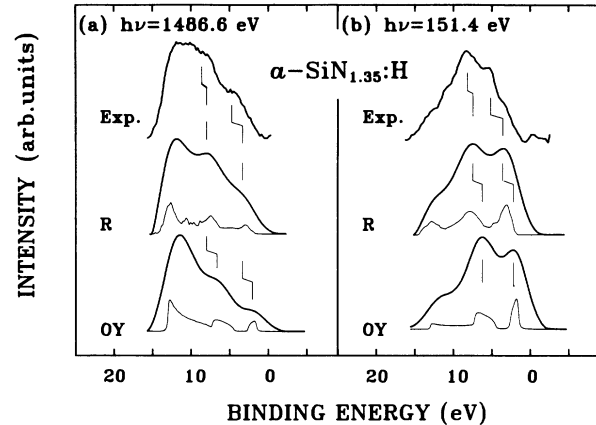


FIG. 6. Same comparison as in Fig. 5 but for a near stoichiometric composition. The experimental spectra correspond to $x = 1.35$ and the calculations to $x = 4/3$.

from *ab initio* total energy Hartree-Fock-self-consistent-field calculations in clusters with the appropriate compositions. We have synthesized photoemission spectra summing the partial DOS's weighted with an average of the cross sections listed in Table II, and convoluting these sums with a Gaussian of 3 eV FWHM representing the combined effects of the instrumental and lifetime broadenings. As at $h\nu = 151.4$ eV all the partial DOS's contributing to the upper VB are summed with approximately equal weights, there is little difference between the synthesized spectra and the total DOS's; therefore, we have used directly the total DOS's to compare with the experiment. The comparisons are made at the two compositions for which experimental and theoretical data (conveniently decomposed into partial DOS's) were available, and restrict to the upper VB's only. A common energy zero was defined by aligning the steep rises of the intensity at ~ 15 eV in the photoemission spectra at $h\nu = 1486.6$ eV.

In Fig. 5 we compare the spectra corresponding to the low N content. Figure 5(a) shows the experimental and calculated photoemission spectra at $h\nu = 1486.6$ eV. Due to its high photoemission cross section, the Si

TABLE II. Photoemission cross sections normalized to that of N 2s.

$h\nu$ (eV)	N 2s	N 2p	Si 3s	Si 3p	Ref.
151.4	1	0.45	0.34	0.31	a
	1	0.44	0.35	0.29	b
	1	0.43	0.35	0.28	c
1486.6	1	0.04	0.88	0.13	a
	1	0.04	0.93	0.14	b
	1	0.03	0.91	0.13	c

^aS.M. Goldberg, C.S. Fadley, and S. Kono, J. Electron. Spectrosc. Relat. Phenom. **21**, 285 (1981).

^bI.M. Band, Yu. I. Kharitonov, and M.B. Trzhaskovskaya, At. Data Nucl. Data Tables **23**, 443 (1979).

^cJ.J. Yeh and I. Lindau, At. Data Nucl. Data Tables **32**, 1 (1985).

3s partial DOS dominates the spectrum with a peak at ~ 10 eV; the other structure near the VBM is formed with contributions from the Si 3p (strong) and N 2p (weak) partial DOS's. There is good agreement in the shape of the bands although the theoretical spectrum is too wide. It is seen that if one aligns the experimental and theoretical Si 3s contributions, the theoretical Si 3p and N 2p contributions appear ~ 1.6 eV too high in energy. Figure 5(b) shows the comparison of the experimental spectrum taken at $h\nu = 151.4$ eV with the total DOS's calculated by R and by OY. Again there is good agreement in the shape of the bands but the peak due to the Si 3p and N 2p contributions near the VBM appear ~ 0.9 eV too high in energy in the calculation of R and ~ 1.2 eV in the calculation of OY.

Similar conclusions can be drawn from the comparisons presented in Fig. 6 corresponding to the near stoichiometric composition. Again the shapes of the spectra are in good agreement, but the theoretical spectra are too wide. In Fig. 6(a) the experimental and theoretical photoemission spectra at $h\nu = 1486.6$ eV are compared. The region around 10 eV is still dominated by the Si 3s contribution, but the more important role played by the N 2p states makes the broad structure near the VBM in Fig. 5(a) split into two other structures: one in the middle of the band due to the Si 3p (weak) and N $2p_{x,y}$ (strong) partial DOS's, and another at the top of the band due to the N $2p_z$ nonbonding states. It is seen that the separation between the Si 3s contribution and the Si 3p and N $2p_{x,y}$ contributions is ~ 0.6 eV too big in the calculation of R, and ~ 2.0 eV too big in the calculation of OY. The separation between the Si 3s and N $2p_z$ contributions is seen to be ~ 1.4 eV too big in the calculation of R and ~ 2.6 eV in the calculation of OY. Figure 6(b) compares the experimental photoemission spectrum taken at $h\nu = 151.4$ eV with the total DOS's calculated by R and by OY. In this comparison the separation between the Si 3s contribution and the Si 3p and N $2p_{x,y}$ contributions is ~ 0.7 eV too big in the calculation of R and ~ 1.9 eV too big in the calculation of OY, whereas the separation between the Si 3s and N $2p_z$ contributions is ~ 1.6

eV too big in the calculation of R and ~ 3.0 eV in the calculation of OY.

IV. CONCLUSIONS

We have measured VB photoemission spectra and dark conductivity of a -SiN $_x$:H films with x between 0 and 1.5. Combining the VBM's derived from the photoemission spectra and the activation energies derived from the dark-conductivity curves with the optical gaps measured previously in this same set of samples we have made a plot of the Fermi level and the band edges as a function of the N content. It is seen that the sudden opening of the gap is due mainly to the recession of the CBM. The correlation observed between the sudden change of the CBM and the falling below one of the mean number of Si neighbors of a Si atom gives experimental support to the interpretation in terms of a percolation transition.

The photoemission spectra taken at $h\nu = 151.4$ eV, which are expected to resemble directly the total DOS's of the alloys, show that the incorporation of N produces a shift of spectral weight from near the VBM towards the center of the VB; this is interpreted as a gradual replacement of Si-Si bonding states by Si-N bonding states. The comparison with the theoretical results has revealed good agreement in the shapes of the bands at both photon energies, 151.4 and 1486.6 eV, but the calculated spectra are too wide; this occurs because the structures due to the Si 3s states, to the Si 3p and N $2p_{x,y}$ states, and to the N $2p_z$ nonbonding states are too separated in energy. The agreement of the theoretical calculations with the experimental spectra is better for Robertson,²⁰ who used tight-binding parameters optimized for this purpose, than for Ordejón and Ynduráin,²¹ who used parameters determined by *ab initio* methods.

ACKNOWLEDGMENTS

We acknowledge the technical assistance of J. de Pellegrin and C. Wenger. H.A. and G.Z. acknowledge CONICET for financial support. We are grateful to P. Ordejón and F. Ynduráin for making available to us their results decomposed into partial DOS.

*Permanent address: UNESP, Departamento de Física, CEP 17033-060 Bauru, SP, Brazil.

¹T. Aiyama, T. Fukunaga, K. Niihara, T. Hirai, and K. Suzuki, *J. Non-Cryst. Solids* **33**, 131 (1979).

²M. Misawa, T. Fukunaga, K. Niihara, T. Hirai, and K. Suzuki, *J. Non-Cryst. Solids* **34**, 313 (1979).

³M. Driss Khodja, A. Le Corre, C. Senemaud, A. Gheorghiu, M.L. Theye, B. Allain, and J. Perrin, *J. Non-Cryst. Solids* **114**, 498 (1989).

⁴H. Kurata, M. Hirose, and Y. Osaka, *Jpn. J. Appl. Phys.* **20**, L811 (1981).

⁵A. Morimoto, Y. Tsujimura, M. Kumeda, and T. Shimizu, *Jpn. J. Appl. Phys.* **24**, 1394 (1985).

⁶S. Hasegawa, T. Tsukao, and P.C. Zalm, *J. Appl. Phys.* **61**, 2916 (1987).

⁷B. Dunnett, D.I. Jones, and A.D. Stewart, *Philos. Mag.* **B 53**, 159 (1986).

⁸A. Iqbal, W.B. Jackson, C.C. Tsai, J.W. Allen, and C.W. Bates, Jr., *J. Appl. Phys.* **61**, 2947 (1987).

⁹L. Yang, B. Abeles, W. Eberhardt, H. Stasiewski, and D. Sondericker, *Phys. Rev. B* **39**, 3801 (1989).

¹⁰R. Kärcher, L. Ley, and R.L. Johnson, *Phys. Rev. B* **30**, 1896 (1984).

¹¹J. Singh and R.C. Budhani, *Solid State Commun.* **64**, 349 (1987).

¹²J.H. Dias da Silva, J.I. Cisneros, F.C. Marques, and M.P. Cantão, in *Current Topics on Semiconductors Physics*, edited by O. Hipolito, A. Fazzio, and G.E. Marques (World Scientific, Singapore, 1988), p. 192.

¹³M.M. Guraya, H. Ascolani, G. Zampieri, J.I. Cisneros, J.H. Dias da Silva, and M.P. Cantão, *Phys. Rev. B* **42**, 5677 (1990).

¹⁴S. Hasegawa, L. He, T. Inokuma, and Y. Kurata, *Phys. Rev. B* **46**, 12478 (1992).

- ¹⁵S.Y. Ren and W.Y. Ching, *Phys. Rev. B* **23**, 5454 (1981).
- ¹⁶J. Robertson, *Philos. Mag.* **44**, 215 (1981); *J. Appl. Phys.* **54**, 4490 (1983); J. Robertson and M.J. Powell, *Appl. Phys. Lett.* **44**, 415 (1984).
- ¹⁷E.C. Ferreira and C.E.T. Gonçalves da Silva, *Phys. Rev. B* **32**, 8332 (1985).
- ¹⁸L. Martín-Moreno, E. Martínez, J.A. Vergés, and F. Ynduráin, *Phys. Rev. B* **35**, 9683 (1987).
- ¹⁹E. San-Fabián, E. Louis, L. Martín-Moreno, and J.A. Vergés, *Phys. Rev. B* **39**, 1844 (1989).
- ²⁰J. Robertson, *Philos. Mag. B* **63**, 47 (1991).
- ²¹P. Ordejón and F. Ynduráin, *J. Non-Cryst. Solids* **137&138**, 891 (1991).
- ²²L. Ley, J. Reichardt, and R.L. Johnson, *Phys. Rev. Lett.* **49**, 1664 (1982).
- ²³Ar atoms were implanted in the samples during the preparation and/or the cleaning process.
- ²⁴F. Alvarez, I. Chambouleyron, C. Constantino, and J.I. Cisneros, *Appl. Phys. Lett.* **44**, 116 (1984).